THE ANTIPROTON SIGNAL OF THE SUPERSYMMETRIC DARK MATTER PRESENT IN THE GALACTIC HALO

PIERRE SALATI
Laboratoire de Physique Théorique LAPTH
BP110, F-74941 Annecy-le-Vieux Cedex, France
E-mail: salati@lapp.in2p3.fr

ABSTRACT

An indirect signature of the presence of particle dark matter in the halo of our Galaxy is an excess of antiprotons at low energy. The 1995 data of the low–energy cosmic–ray $\bar{p}$ spectrum, that have been published by the BESS Collaboration, are presented here in the light of newly calculated fluxes for secondary antiprotons. The possible contribution of an exotic signal due to neutralino annihilation is analyzed. The supersymmetric configurations that are compatible with the BESS results are derived [1)]. Once the energy spectrum of the secondary $\bar{\mathrm{p}}$ component is well understood, measurements of the antiproton cosmic–ray flux at the Earth will be a powerful probe of the existence of supersymmetric relics in the galactic halo. Unfortunately, that spallation background is still spoilt by considerable theoretical uncertainties. Searches for low–energy antideuterons appear in the mean time as a plausible alternative [2)], worth being explored. Above a few GeV/n, a dozen spallation antideuterons should be collected by the future AMS experiment on board ISSA. For energies less than ~ 3 GeV/n, the $\bar{\mathrm{D}}$ spallation component becomes negligible and may be supplanted by a possible supersymmetric signal. If a few low–energy antideuterons are discovered, this should be seriously taken as a clue for the existence of massive neutralinos in the Milky Way.

1. Hints for a non-baryonic dark matter.

A large fraction of the mass in the Universe still remains invisible. That so-called dark matter is one of the enigma which has been puzzling astronomers for more than half of a century and is yet to be understood. Flat galactic rotation curves, large dispersion velocities inside clusters of galaxies as well as new X-ray determinations of the mass of the latter suggest, as a few other indications, the presence of large amounts of unseen material whose nature is still to be determined. In the halo surrounding our own Galaxy, the popular wisdom has put stellar compact objects forward as candidates for the dark matter. However, with a mass ranging from ~ 0.3 to $1\ M_{\odot}$, that solution is not satisfactory. Actually, if such stars pervade the neighborhood of the Milky Way, they must have died by now, hence massive progenitors. However, those heavy stars must not have enriched the surrounding interstellar medium with heavy elements. A bizarre initial mass function, unnaturally peaked around $3\ M_{\odot}$, can reconcile these two contradictory requirements. More interesting is the recent observation of gravitational microlensing events in the direction of the LMC and SMC where the lens is a binary system. In that case, the position of the lens may be determined on the line of sight from the timing of the caustic crossings. In all cases, the lenses were located within the LMC or SMC. There are now ongoing studies whose aim is to explain the observed optical depth of $\sim 10^{-7}$ in terms of self-lensing by these galaxies

[3,4]. Another possibility is the existence of clouds of cold molecular hydrogen, undetectable with radio-telescopes. However, such clouds cannot populate the immediate vicinity of our Galaxy without interacting with high–energy cosmic–rays and, as a consequence, without shining as sources of a noticeable gamma-ray diffuse background [5].

Studies of the X-ray hot gas that fills up clusters of galaxies show that most of the mass lying in these systems could have a non-baryonic origin. Actually, large clusters of galaxies, such as Virgo or Fornax, contain gas that is sufficiently hot, *i.e.*, with a typical temperature $T \sim 10^7 - 10^8$ K, to radiate a strong X-ray emission. Allowing for the intensity and energy spectrum of the latter, the temperature and density distributions of the inner-cluster gas may be inferred. The gas is believed to be roughly in hydrostatic equilibrium. Its temperature is in general close to the virial temperature derived from the dispersion velocity of the galaxies inside the cluster. Assuming that hydrostatic equilibrium holds, the inner distribution of the total mass may be directly determined from the X-ray luminosity profile. The contribution of the hot gas to the total mass turns out to be larger than expected. An analysis by G. Evrard [6] shows that the gas fraction is on average equal to

$$F_{\rm gas} \; = \; (0.060 \pm 0.003) \; h^{-3/2} \simeq 0.13 \;\; , \tag{1}$$

for a Hubble constant $h = 0.6$. Because clusters of galaxies are actually very large systems, extending on several Mpc, this gas fraction is believed to be representative of the cosmological baryonic contribution to the mass density of the Universe

$$F_{\rm gaz} \simeq \frac{\Omega_{\rm B}}{\Omega_{\rm m}} \;\; . \tag{2}$$

This line of reasoning points towards a consistent scenario with a cosmological matter abundance $\Omega_{\rm m} \sim 0.3$ together with a baryon density $\Omega_{\rm B} \sim 0.04$. That value corresponds to a baryon-to-photon ratio of $\eta_{10} \sim 4$ and is in agreement with the low abundance of primordial deuterium as inferred by Tytler *et al.* [7]. The hot X-ray gas would be therefore the major component of the baryonic content of galactic clusters. The latter would be predominantly made of non-baryonic dark matter.

One of the favourite candidates to the astronomical missing mass is a neutral weakly interacting particle. Such a species is predicted in particular by supersymmetry, a theory that is actively tested at accelerators. There are indirect clues for supersymmetry, noticeably the existence of a single high-energy unification scale for supersymmetric grand-unified models alone. It is conceivable therefore that most of the dark matter in the halo of our own Galaxy is made of such neutral particles. The relic abundance of these so-called neutralinos is relevant to cosmology. If present in the galactic halo, they should still annihilate mutually to yield, among a few other indirect signatures, a flux of antiprotons whose spectrum, at low energy, should exceed the flux of secondary spallation antiprotons.

Statistically significant experimental information on low–energy cosmic–ray antiprotons will soon be made available by ongoing and forthcoming [8] experiments: the BESS balloon–borne measurements [9], AMS on the precursor Shuttle flight of June 1998 and on the International Space Station Alpha (ISSA) in 2003 [10] and the satellite–borne PAMELA experiment [11]. It is therefore crucial to investigate in detail the production of antiprotons throughout our Galaxy and to ascertain which of the spallation of high–energy cosmic–ray protons or of the possible neutralino annihilation is dominant below ~ 1 GeV. The former process is briefly reviewed in Sec. 2. The latter mechanism is discussed in Sec. 3, in the light of the 1995 BESS results. It is not clear whether the supersymmetric antiprotons dominate or not over the spallation background. In the case of antideuterons, the spallation component is actually negligible at low energies. The secondary and supersymmetric antideuteron fluxes will be discussed in Sec. 4 while future prospects and conclusions will be drawn in Sec. 5.

2. Secondary antiprotons.

Antiprotons are naturally produced by the nuclear interactions of cosmic–ray particles with the interstellar medium. Since both cosmic–rays and the interstellar medium are mostly composed of protons, the fundamental process is the collision or spallation of a high-energy proton with a proton at rest in the interstellar medium. This reaction produces hadrons, mostly pions whose radiative decays are the principal source of the galactic diffuse gamma-ray emission. During the fragmentation process, when the inelastic collision produces coloured strings, resonances such as Λ^0, Δ^-, Δ^{--} or Σ^- are formed and subsequently decay into antiprotons and antineutrons, the latter decaying in turn into antiprotons. The threshold for the antiproton production mechanism $p+p \to 3p+\overline{p}$ is 7 GeV. The antiproton multiplicity per collision is defined as

$$Y_{\bar{\mathrm{p}}}(E_{\mathrm{p}} \to E_{\bar{\mathrm{p}}}) \;=\; \frac{dN_{\bar{\mathrm{p}}}}{dE_{\bar{\mathrm{p}}}} \;\;, \tag{3}$$

where E_{p} stands for the energy of the incoming cosmic–ray proton while $E_{\bar{\mathrm{p}}}$ denotes the energy of the resulting antiproton. That multiplicity obtains from the appropriate integral over phase space of the Lorentz invariant antiproton production cross section $E_{\bar{\mathrm{p}}}\, d^3\sigma/d^3P_{\bar{\mathrm{p}}}$ as parametrized by Tan and Ng [12].

As suggested by Parker, the propagation of cosmic–rays inside the Galaxy is strongly affected by their scattering on the irregularities of magnetic fields. This results into a diffusive transport. In the following, we will assume an isotropic diffusion with an empirical value for the diffusion coefficient. A valuable hint for the existence of a diffusion region in our Galaxy is provided by diffuse γ-ray observations [13,14], which point towards the presence of cosmic–rays far above the galactic disk. Our Galaxy can be reasonably well modelled by a thin disk of atomic and molecular hydrogen with $0 \leq r \leq R \;=\; 20$ kpc and $|z| \leq h \;=\; 100$ pc, associated to an extended region of diffusion containing irregular magnetic fields with the same radial extension and $|z| \leq L = 3$ kpc. Those various regions are superimposed to the spheroidal halo of dark matter whose density profile will be given in the next section. That two–zone diffusion model is in good agreement with the observed primary and secondary nuclei abundances [15]. Since their discovery by Golden in 1979 [16], cosmic antiprotons have been thoroughly studied in the framework of the leaky box model

[17]. We analyse here their propagation throughout the Galaxy in the light of a two–zone diffusion model [1,18].

In a stationary regime, the propagation equation of cosmic antiprotons may be expressed as

$$\frac{\partial n_{\bar{\mathrm{p}}}}{\partial t} \; = \; 0 \; = \; K \Delta n_{\bar{\mathrm{p}}} \; - \; \Gamma_{\bar{\mathrm{p}}} \, n_{\bar{\mathrm{p}}} \; - \; \frac{\partial}{\partial E} \left\{ b(E) n_{\bar{\mathrm{p}}} \right\} \; + \; q_{\bar{\mathrm{p}}} \;\; , \tag{4}$$

where $n_{\bar{\mathrm{p}}}(E_{\bar{\mathrm{p}}}, r, z)$ is the density of antiprotons with energy $E_{\bar{\mathrm{p}}}$ at location (r, z). In the right-hand side of relation (4), the first term describes the diffusion of antiprotons. The diffusion coefficient K is constant at low energy, but raises with the rigidity p of the particle beyond a critical value of 1 GV. This behaviour can be modelled by the form

$$K \; = \; 6 \times 10^{23} \; \mathrm{m^2 s^{-1}} \; \left(1 + \frac{p}{1 \; \mathrm{GV}} \right)^{0.6} \quad . \tag{5}$$

Based on that value, we have estimated the grammage Λ_e which the CNO elements cross

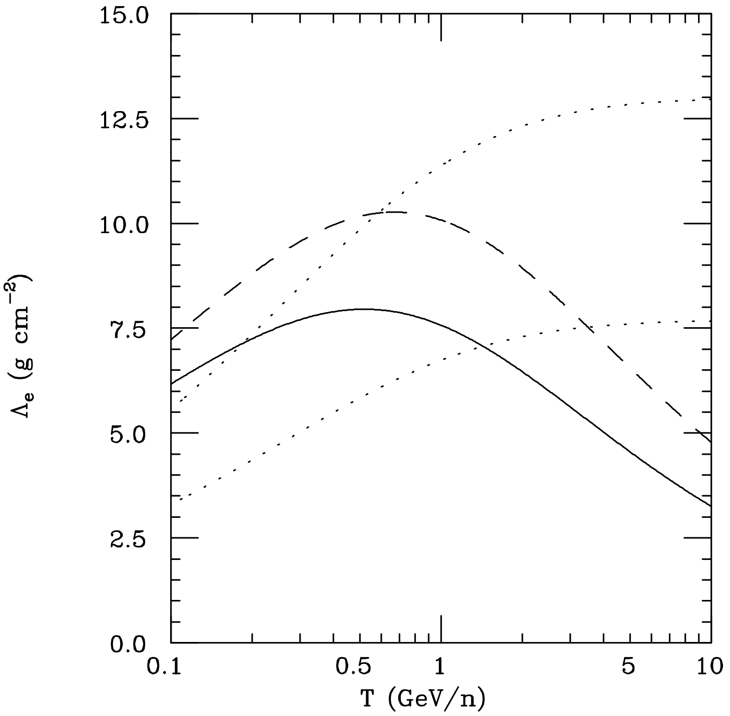

Figure 1: The grammage Λ_e of the CNO primary elements (solid) as inferred from a two–zone diffusion model of the propagation of cosmic–rays in the Galaxy. It is plotted as a function of the kinetic energy per nucleon. The dashed curve features the grammage corresponding to antiprotons while the dotted lines delineate the interval of escape lengths inferred from the Ficenec *et al.* [19] observations on ^{3}He at TOA energies comprised between 100 MeV/n and 1.6 GeV/n.

during their journey inside the galactic disk. It is plotted in Fig. 1 as a function of the kinetic energy per nucleon (solid line). It reaches a maximum of ~ 8 g cm^{-2} at 500 MeV/n.

It decreases at low energies with the velocity. It also drops at high energies as a result of a better diffusion and hence a lower time of residence in the disk. The dashed curve refers to the grammage of the antiprotons. At fixed kinetic energy, the diffusion coefficient is slightly smaller for these species than for heavier elements, hence a larger escape length Λ_e. Ficenec *et al.* [19] have taken data on ^{3}He between 100 MeV/n and 1.6 GeV/n. They conclude that the grammage of primary cosmic–rays is well fitted by $\Lambda_e = (10.5 + 2.5 - 2.8)\ \beta$ g cm^{-2}. The extreme values of that fit are featured by the dotted curves of Fig. 1. The CNO grammage inferred from our two–zone model lies in the range of escape length delineated by the Ficenec *et al.* extreme values, for energies in interstellar space comprised between 200 MeV/n and 1.5 GeV/n. The second term in Eq. (4) describes the destruction of antiprotons by their interactions with the interstellar medium. That destruction rate is shown to be very small but has not been neglected in what follows. The collision rate of antiprotons with the interstellar hydrogen is given by

$$\Gamma_{\bar{\mathrm{p}}} \; = \; \sigma_{\bar{\mathrm{p}}\mathrm{H}} \; v_{\bar{\mathrm{p}}} \; n_{\mathrm{H}} \quad , \tag{6}$$

where $\sigma_{\bar{\mathrm{p}}\mathrm{H}}$ is the total antiproton interaction cross section with protons, $v_{\bar{\mathrm{p}}}$ denotes the velocity and $n_{\mathrm{H}} = 1$ cm^{-3} is the average hydrogen density in the thin matter disk. The third term in relation (4) stands for the energy losses suffered by the antiproton cosmic–rays while they propagate in the galactic disk. That term actually exists for any cosmic–ray species. Because the particle fluxes do not significantly drop at low energies, this effect is in general neglected. In the specific case of secondary antiprotons, that is no longer valid. Because a high energy proton has very little chance to produce an antiproton at rest while colliding on an hydrogen atom, the secondary antiproton flux sharply drops when the energy decreases below ~ 1 GeV. Energy losses tend to shift the antiproton spectrum towards lower energies with the effect of replenishing the low energy tail with the more abundant species which had initially a higher energy. The last term in relation (4) deals with the source of antiprotons. Those particles are produced by the spallation of cosmic protons on the interstellar matter of the disk. The antiproton production rate involves a convolution over the incident cosmic proton energy spectrum $dn_{\mathrm{p}}/dE_{\mathrm{p}}$

$$q_{\bar{\mathrm{p}}}^{\mathrm{st}}(E_{\bar{\mathrm{p}}}) \; = \; \int_{E_{\bar{\mathrm{p}}}}^{+\infty} dE_{\mathrm{p}} \; \left\{ \frac{dn_{\mathrm{p}}}{dE_{\mathrm{p}}}(E_{\mathrm{p}}) \right\} \; \Gamma_{\mathrm{p}}(E_{\mathrm{p}}) \; Y_{\bar{\mathrm{p}}}(E_{\mathrm{p}} \rightarrow E_{\bar{\mathrm{p}}}) \quad . \tag{7}$$

The collision rate Γ_{p} of protons with the interstellar gas is defined in just the same way as the collision rate $\Gamma_{\bar{\mathrm{p}}}$ of antiprotons in relation (6). The antiproton differential spectrum $Y_{\bar{\mathrm{p}}}$ produced during a single proton spallation was previously defined in Eq.(3).

We have solved Eq.(4) following the analysis by Webber, Lee and Gupta [15]. At the edge of the domain where cosmic–rays are confined, the particles escape freely and the diffusion becomes inefficient. Thus the density vanishes at the boundaries of the domain where cosmic–rays are confined by diffusion. This provides the initial conditions for solving the diffusion equation. Then, because the problem has a cylindrical symmetry, the densities n_{p} and $n_{\bar{\mathrm{p}}}$ may be expanded as a series of the Bessel functions of zeroth order $J_0\,(\zeta_i x)$ where

ζ_i is the ith zero of J_0 and where $x = r/R$. Details may be found in [1,18]. The cosmic–ray sources are located in the thin gaseous disk and we have taken the radial distribution of supernovae remnants and pulsars measured by Lyne *et al.* [20]. As regards the spallation mechanism, suffice it to say that an effective antiproton multiplicity may be defined as

$$Y_{\bar{\rm p}}^{\rm eff}(E_{\bar{\rm p}}) \;=\; \int_{E_{\bar{\rm p}}}^{+\infty} dE_{\rm p} \left\{ \frac{\Phi_{\rm p}(E_{\rm p})}{\Phi_{\rm p}(E_{\bar{\rm p}})} \right\} Y_{\bar{\rm p}}(E_{\rm p} \rightarrow E_{\bar{\rm p}}) \;\;, \tag{8}$$

so that no convolution with the cosmic proton energy spectrum is needed any longer. The differential flux $dn_{\rm p}/dE_{\rm p}$ of protons of energy $E_{\rm p}$ is denoted here by $\Phi_{\rm p}(E_{\rm p})$.

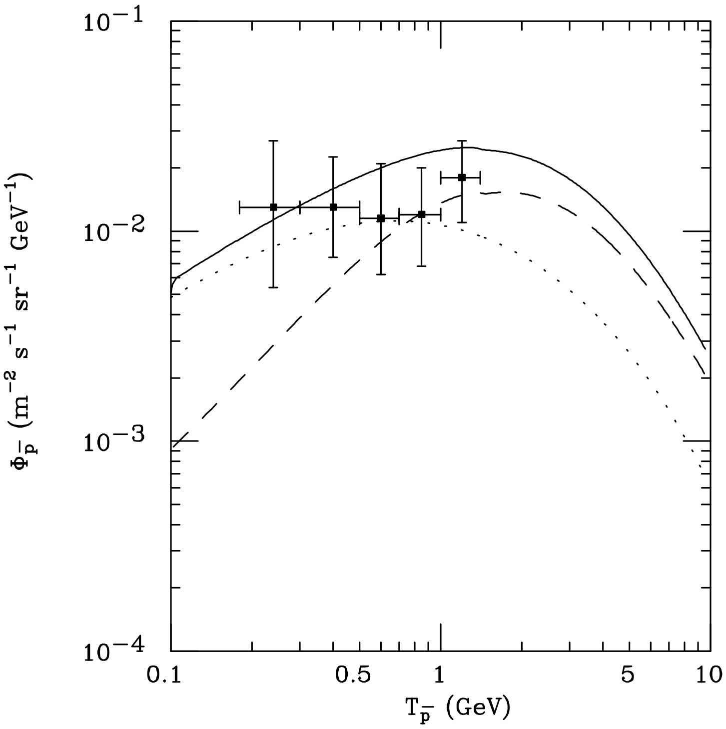

Figure 2: TOA antiproton fluxes versus the antiproton kinetic energy [1]. The BESS data [9] are shown by crosses. The dashed line denotes the secondary flux produced by spallation, the dotted one features the primary flux due to neutralino annihilation in the halo for a neutralino configuration with $m_\chi = 62$ GeV, $P = 0.98$ and $\Omega_\chi h^2 = 0.11$. The solid line denotes the calculated total flux.

The resulting secondary antiproton flux is featured [1] by the dashed line in Fig. 2 where different top of the atmosphere (TOA) fluxes are plotted as a function of the antiproton kinetic energy. It may be compared to the BESS data [9] as shown by the crosses. There seems to be a small excess at low energy, precisely the region where an exotic signal may show up. However, note that the data points are well fitted by the secondary flux alone, with a reduced χ^2 of 0.83.

3. BESS95 and supersymmetric antiprotons.

The dark matter halo that makes up the most massive (yet invisible) component of our Galaxy could be made of neutralinos. These are particles predicted by supersymmetry, an extension of the Standard Model of particle physics. The possibility to detect the presence of neutralinos in our galactic halo has been extensively studied in many different ways [21]. When neutralinos encounter in the Galaxy, they annihilate into antiprotons, among other products. These extra antiprotons would contribute to those already observed in cosmic–rays, thus giving rise to an experimental deviation to the spectrum computed above.

The differential rate (per unit volume and per second) for the production of antiprotons from χ–χ annihilations is given by

$$q_{\bar{\mathrm{p}}}^{\mathrm{susy}}(E_{\bar{\mathrm{p}}}) \; = \; \langle \sigma v \rangle \, f(E_{\bar{\mathrm{p}}}) \, \left\{ \frac{\rho_\chi}{m_\chi} \right\}^2 \quad , \tag{9}$$

in which $\langle \sigma v \rangle$ is the χ–χ annihilation cross section averaged over the relative velocities of the reacting neutralinos. For a single annihilation, the antiproton energy spectrum is

$$f(E_{\bar{\mathrm{p}}}) \; \equiv \; \frac{1}{\sigma} \, \frac{d\sigma(\chi\chi \to \bar{\mathrm{p}} + X)}{dE_{\bar{\mathrm{p}}}} \; = \; \sum_{F,f} B_{\chi f}^{(F)} \left(\frac{dN_{\bar{\mathrm{p}}}^f}{dE_{\bar{\mathrm{p}}}} \right) \quad , \tag{10}$$

where F describes the χ–χ annihilation final state and $B_{\chi f}^{(F)}$ is the branching ratio into the quarks or gluons f in the channel F. The differential distribution of the antiprotons generated by the hadronization of quarks (with the exception of the top quark) and of gluons is denoted by $dN_{\bar{\mathrm{p}}}^f/dE_{\bar{\mathrm{p}}}$ and depends on the nature of the species f. Of the various quantities that are present in Eq.(9), $\langle \sigma v \rangle$ and $f(E_{\bar{\mathrm{p}}})$ depend on the neutralino properties. The antiproton production rate also depends on the distribution ρ_χ of the dark matter particles inside the galactic halo.

The neutralino annihilation cross section $\langle \sigma v \rangle$ is evaluated as in Ref. [1,18]. The minimal supersymmetric standard model is defined at the electroweak scale as a straightforward supersymmetric extension of the Standard Model. The Higgs sector consists of two Higgs doublets H_1 and H_2, which define two free parameters : the ratio of the two vacuum expectation values $\tan\beta \equiv \langle H_2 \rangle / \langle H_1 \rangle$ and the mass m_A of the neutral pseudoscalar Higgs. The other parameters of the model are contained in the superpotential, which includes all the Yukawa couplings and the Higgs–mixing term $\mu H_1 H_2$, and in the soft–breaking Lagrangian, which includes the trilinear and bilinear breaking parameters and the soft gaugino and scalar mass terms. For details, we refer the reader to the above cited analysis. The parameter P describes the nature of the neutralino. The closer to unity, the more gaugino like.

The neutralino halo distribution ρ_χ is taken to be spherically symmetric. In the axisymmetric coordinate system r and z, the density profile is given by

$$\rho_\chi(r,z) \;=\; \rho_\chi(\odot)\,\left\{\frac{a^2+r_\odot^2}{a^2+r^2+z^2}\right\}\;, \tag{11}$$

where $a = 3.5$ kpc is the core radius of the dark matter halo.

The supersymmetric source term for antiprotons is then plugged in the diffusion model described in the previous section. The resulting supersymmetric antiproton flux in cosmic–rays corresponds to the dotted curve of Fig. 2. A specific choice of supersymmetric parameters has been assumed here. It corresponds to a neutralino with a mass $m_\chi = 62$ GeV that contributes a cosmological relic density of $\Omega_\chi h^2 = 0.11$. That species is mostly a gaugino with $P = 0.98$, *i.e.*, in that case the supersymmetric Majorana fermion associated to the photon and the Z^0 boson. The solid line corresponds to the total flux that takes into account both the spallation secondary antiprotons and the supersymmetric antiprotons. Because the latter are produced at rest in the annihilation of a neutralino pair, the corresponding low–energy spectrum tends to be flat and exceeds the spallation signal.

As is clear from Fig. 2, the agreement between the BESS experimental data and theory may be improved by adding a fraction of neutralino–induced $\bar{p}$'s to the standard secondary antiprotons. The best fit to the experimental data with a total theoretical flux $\Phi^{\rm th} = \Phi^{\rm sec}_{\rm med}$ $+\ \Phi^{\rm susy}$, performed by varying the supersymmetric parameters provides a value of 0.28 for the reduced χ^2, with an improvement with respect to the case where spallation antiprotons are alone. This fact cannot certainly be taken as significant of an evidence of a neutralino–induced antiproton signal. It nevertheless indicates that the low–energy region $\bar{p}$ spectrum is a quite interesting window to explore.

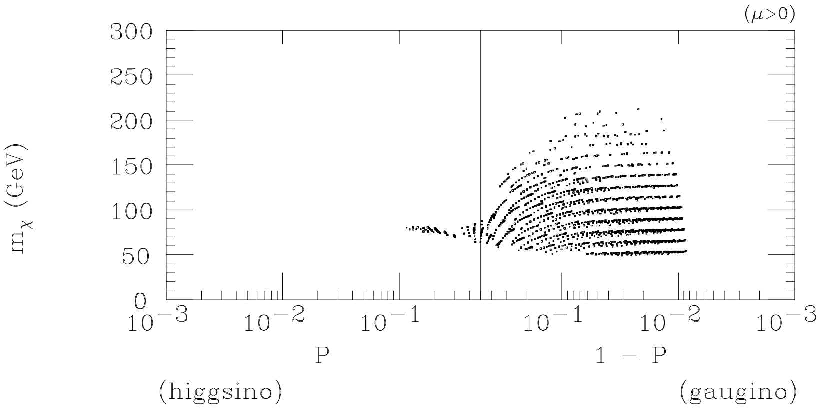

Figure 3: Scatter plots for the supersymmetric configurations that are compatible with the BESS data. Points are drawn in the P–m_χ plane. Most of the configurations are gaugino–like.

The supersymmetric parameter space has been surveyed [1)] in the light of the BESS results. Relevant supersymmetric configurations have been selected according to three requirements. First, the supersymmetric antiproton flux must be in agreement with the experimental data, with a reduced χ^2 less than a maximal value of 2.2, corresponding to 95% C. L. for 5 data points. Then, the relic abundance of the neutralino is required to be of cosmological relevance, with $\Omega_\chi h^2$ lying in the range from 0.03 to 0.7. Finally, configurations for which the primary supersymmetric antiproton flux is too small have been removed from our selection. The total theoretical flux $\Phi^{\rm th}$ is required to be at least at the level of the experimental value (within 1–σ) in the first energy bin. The resulting set of configurations is presented as a constellation of points in the P–m_χ plane of Fig. 3. Most of the configurations are gaugino–like. At fixed mass, gauginos tend to annihilate more efficiently than higgsinos. The relic abundance of gauginos is therefore relevant to cosmology for a range of neutralino masses which, very crudely, tends to be smaller than in the higgsino case. Notice that the heavier the particle, the less abundant today at fixed galactic density and the fewer the ongoing annihilations.

For light gauginos, we therefore expect a very strong antiproton signal. Fig. 4 features these configurations for which the total antiproton flux $\Phi^{\rm th}$ is so large that the corresponding reduced χ^2 exceeds a value of 4. Such configurations are excluded by the BESS data at the 99.9 % C.L. If the dark matter halo that surrounds our Milky Way is a flattened spheroid,

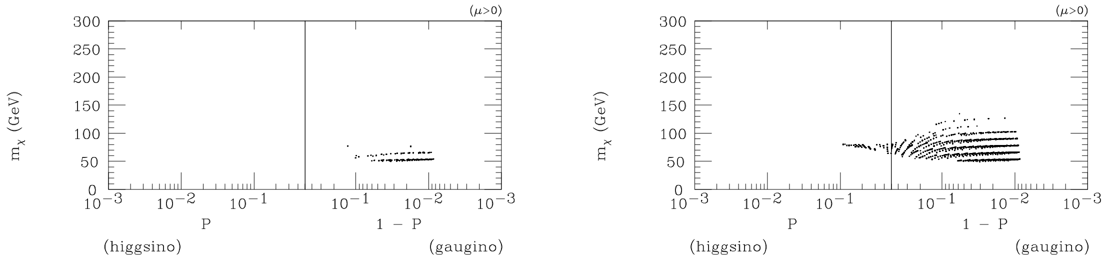

Figure 4: The supersymmetric configurations for which the reduced $\chi^2 > 4$ are excluded by the BESS data. They are plotted in the P–m_χ plane. Notice that they correspond to light gauginos. In the `left` pannel, the neutralino halo is assumed to be spherical whereas in the `right` pannel, a flattening factor $f = 0.5$ has been taken into account. In this case, the halo is more compressed along the vertical axis, the neutralino density and annihilation are enhanced, hence a larger antiproton signal. The BESS data therefore exclude more configurations than in the pure spherical case.

the density of neutralinos inside our Galaxy is enhanced as a result of compression along the vertical axis. The supersymmetric antiproton flux increases and the BESS data turn out to be more stringent than in the pure spherical case. The effect of a halo flattening on the excluded supersymmetric configurations is presented in Fig. 4. The flattening factor $f = 0.5$ corresponds to a contraction of the vertical scale by a factor of 2. There are more excluded configurations as a result of an enhanced ongoing neutralino annihilation. They still mostly correspond to gauginos, with now a small admixture of higgsinos.

In Fig. 5, the 90 % C.L. experimental [22] upper bound (open solid line) on the neutralino–nucleon scalar cross–section $\sigma_{\rm scalar}^{\rm nucleon}$ is presented as a function of the neutralino mass. The factor ξ is the actual neutralino density in the solar neighborhood expressed in units of 0.4

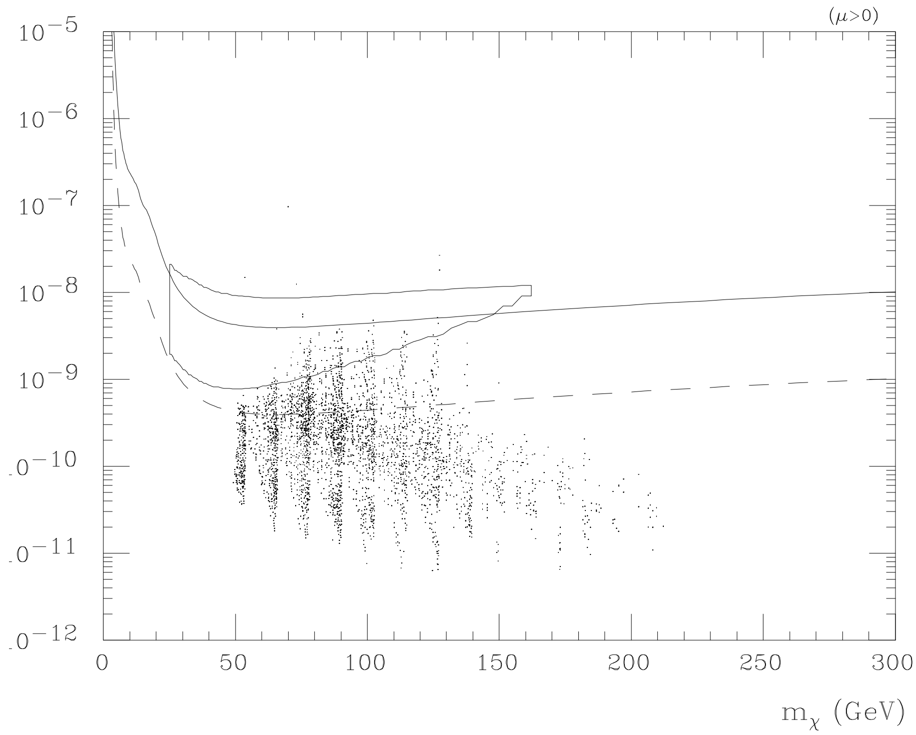

Figure 5: Scatter plot of the values of $\xi\sigma^{\rm nucleon}_{\rm scalar}$ versus neutralino mass for the set of configurations featured in Fig. 3. The open solid curve denotes the 90 % C.L. upper bound obtained from direct detection experiments while the dashed line presents the discovery potential in case of an improvement by a factor of 10 in current sensitivities.

GeV cm^{-3}. The region in Fig. 5 delimited by a closed contour is the one singled out by the experiment of Ref. [23)] as possibly indicative of an annual modulation effect. The scatter plot displays the values of $\xi\sigma^{\rm nucleon}_{\rm scalar}$ for the supersymmetric configurations delineated in Fig. 3. A sizeable fraction of the configurations are accessible to investigation by direct detection, since the sensitivity in this kind of experiments is expected to be significantly improved in the near future (open dashed line).

4. Antideuterons as a new probe for neutralinos.

There is quite an excitement trying to extract from the observations a possible $\bar{\rm p}$ exotic component which would signal the presence of supersymmetric dark matter in the Galaxy. In principle, supersymmetric antiprotons should be abundant at low energy, a region where the flux of $\bar{\rm p}$ secondaries is a priori negligible. Unfortunately, it has been recently realized [1,24,25)] that a few processes add up together to flatten out, at low energy, the spectrum of secondary antiprotons. Ionisation losses as well as inelastic but non-annihilating scatterings on the hydrogen atoms of the galactic disk result into the decrease of the antiproton energy. The low–energy tail of the $\bar{\rm p}$ spectrum is replenished by the more abundant population from higher energies. That effect is further strengthened by solar modulation which also shifts the energy spectrum towards lower energies. As a result of these effects, the secondary $\bar{p}$'s are much more abundant at low energy than previously thought. Disentangling an exotic supersymmetric contribution from the conventional component of spallation antiprotons may turn out to be a very difficult task. The antiproton signal of supersymmetric dark matter seems therefore in jeopardy.

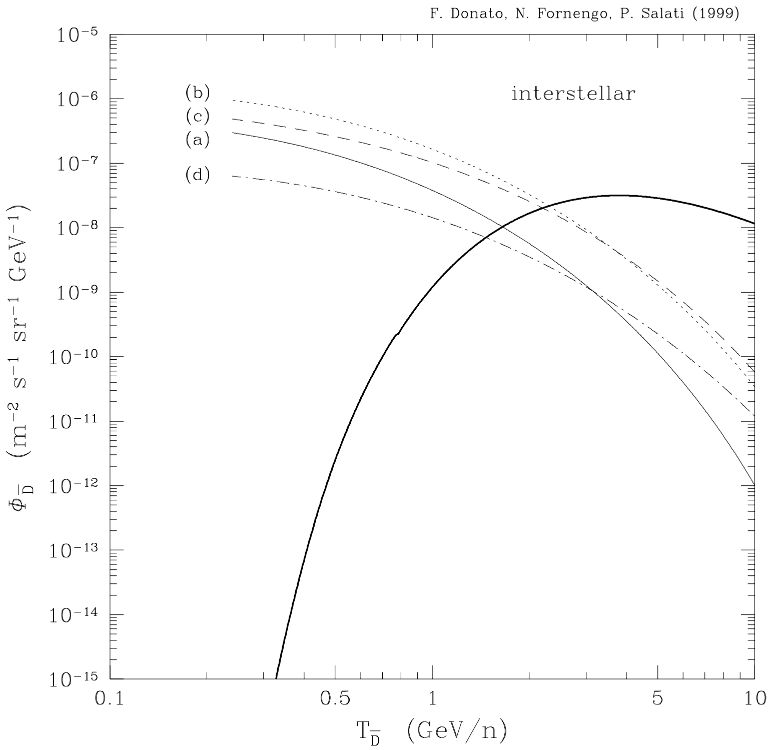

Figure 6: The IS flux of secondary antideuterons (heavier solid curve) decreases at low energy whereas the energy spectrum of the antideuterons from supersymmetric origin tends to flatten. The four cases discussed in Ref. [2] are respectively featured by the solid (a), dotted (b), dashed (c) and dot-dashed (d) curves.

Antideuterons, *i.e.*, the nuclei of antideuterium, are free from such problems. They form when an antiproton and an antineutron merge together. The two antinucleons must be at rest with respect to each other in order for fusion to take place successfully. For kinematic reasons, a spallation reaction creates very few low–energy particles. Low-energy secondary antideuterons are even further suppressed. Energy loss mechanisms are also less efficient in shifting the antideuteron energy spectrum towards low energies. The corresponding interstellar (IS) flux reaches a maximum of $2-5 \times 10^{-8}$ $\bar{\rm D}$ m^{-2} s^{-1} sr^{-1} GeV^{-1} for a kinetic energy of $\sim$ 4 GeV/n. A dozen of secondary antideuterons should be collected by the AMS/ISSA experiment.

On the other hand, supersymmetric $\bar{\rm D}$'s are manufactured at rest with respect to the

Galaxy. In neutralino annihilations, antinucleons are predominantly produced with low energies. This feature is enhanced by their subsequent fusion into antideuterons, hence a fairly flat spectrum for supersymmetric antideuterium nuclei as shown in Fig. 6. Below a few GeV/n, secondary antideuterons are quite suppressed with respect to their supersymmetric partners. That low–energy suppression is orders of magnitude more effective for antideuterons than for antiprotons. This makes cosmic–ray antideuterons a much better probe of supersymmetric dark matter than antiprotons.

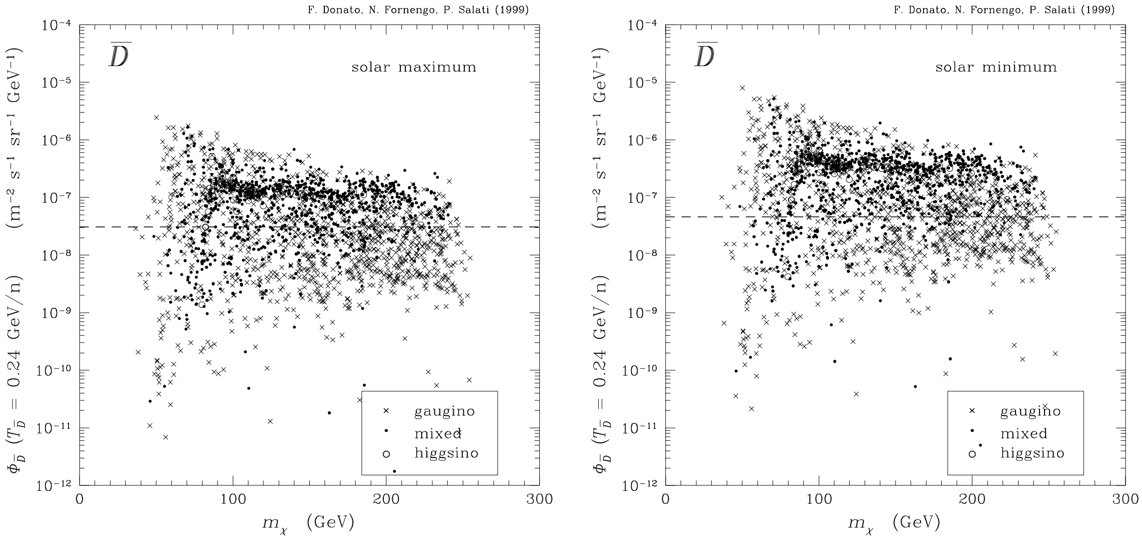

Figure 7: Scatter plots in the plane m_χ–$\Phi_{\bar{\rm D}}^{\rm TOA}$. The Earth antideuteron flux $\Phi_{\bar{\rm D}}^{\rm TOA}$ has been computed at solar maximum (`left`) and minimum (`right`), for a modulated energy of 0.24 GeV/n. Configurations lying above the horizontal lines correspond to the detection of at least one antideuteron in the range of interstellar energies 0.1 – 3 GeV, by an experiment of the AMS caliber on board ISSA.

Unfortunately, antideuteron fluxes are quite small with respect to p̄'s. We have nevertheless shown [2)] that a significant portion of the supersymmetric parameter space may be explored by measuring the cosmic–ray D̄ flux at low energy. In particular, an AMS/ISSA caliber experiment should reach a sensitivity of 4.8×10^{-8} D̄ m^{-2} s^{-1} sr^{-1} GeV^{-1} at solar minimum, pushing it down to 3.2×10^{-8} D̄ m^{-2} s^{-1} sr^{-1} GeV^{-1} at solar maximum, for a modulated energy of 0.24 GeV/n.

5. Future prospects.

Precise measurements of the antiproton spectrum at low energy are crucial to disentangle the secondary $\bar{p}$ flux from a possible primary signal of exotic nature. Satellite observations such as AMS or PAMELA as well as balloon–borne experiments like BESS should clarify matters. A word of caution is nevertheless mandatory at this stage. The theoretical determination of the secondary $\bar{p}$ contribution is still affected by a few uncertainties. To commence, the difficulty to measure accurately the proton flux itself translates into a shift on the antiproton signal by $\pm 25\%$. The diffusion coefficient K also adds up a mere $\pm 45\%$ at low energies (100 MeV) and $\pm 20\%$ at larger ones (above 0.6 GeV). This uncertainty may be reduced by including the light elements. Measurements of the B/C ratio should allow for a better determination of K at low energy [26)]. Then, antiproton energy losses need to be taken into account. Finally, the possibility of diffusive reacceleration [27,28,29)] should be considered at some point. That second order Fermi mechanism could occur in the gaseous disk of our Galaxy. It would lead to the increase of the averaged antiproton energy. It would also result into the $\bar{p}$ spectrum spreading in energy, with the consequence of further repleneshing the low–energy states. Finally, cosmic–ray proton collisions on the nuclei of the interstellar medium as well as interactions of high–energy nuclei with that gas should also be considered. It is not yet clear that such processes are negligible as shown by a recent Monte Carlo simulation [30)] and by Ref. [24)].

Supersymmetric antiprotons are four orders of magnitude more abundant in cosmic–rays than antideuterons. However, they may be swamped in the background arising from the secondaries. The AMS experiment will collect a large number of antiprotons on board ISSA. Our concern is whether an hypothetical supersymmetric $\bar{\mathrm{p}}$ signal may be disentangled from the background. Because the latter still suffers from large theoretical uncertainties, we are afraid that antiproton searches in cosmic–rays are not yet the ultimate probe for the existence of supersymmetric relics in the Milky Way. As discussed in Refs. [1,24,25)], the distribution of secondary antiprotons turns out to be flatter than previously estimated. Therefore, it is still a quite difficult task to ascertain which fraction of the measured antiproton spectrum may be interpreted as a supersymmetric component. Meanwhile, searches for low–energy antideuterons appear as a plausible alternative, worth being explored. Above a few GeV/n, a dozen spallation antideuterons should be collected by the future AMS experiment on board ISSA. For energies less than $\sim$ 3 GeV/n, the $\bar{\mathrm{D}}$ spallation component becomes negligible and may be supplanted by a possible supersymmetric signal. If a few low–energy antideuterons are discovered, this should be seriously taken as a clue for the existence of massive neutralinos in the Milky Way.

6. Acknowledgements

P. S. would like to thank Professor Milla Baldo Ceolin as well as the organizers of the 8^{th} *International Workshop on Neutrino Telescopes* for their very kind hospitality and for this very nice and inspiring Conference.

7. References

1) A. Bottino, F. Donato, N. Fornengo and P. Salati, *Phys. Rev.* **D58** (1998) 123503 .
2) F. Donato, N. Fornengo and P. Salati, preprint lapth–722/99 and FTUV/99-9 and `hep-ph/9904481`, submitted to *Physical Review* **D**.

3) É. Aubourg, N. Palanque-Delabrouille, P. Salati, M. Spiro and R. Taillet, preprint lapth–721/99 and `astro-ph/9901372`, accepted for publication in *Astronomy & Astrophysics.*
4) P. Salati, R. Taillet, É. Aubourg, N. Palanque-Delabrouille and M. Spiro, preprint `astro-ph/9904400`, submitted to *Astronomy & Astrophysics.*
5) P. Salati, P. Chardonnet, X. Luo, J. Silk and R. Taillet, Astrononomy & *Astrophysics* **313** (1996) 1 .
6) The intracluster gas fraction in X-ray clusters : constraints on the clustered mass density; G. Evrard, preprint `astro-ph/9701148`, submitted to *MNRAS.*
7) S. Burles and D. Tytler, preprint `astro-ph/9803071`, to appear in the *Proceedings of the Second Oak Ridge Symposium on Atomic & Nuclear Astrophysics* OakRidge TN editor Mezzacappa A (Institute of Physics, Bristol).
8) P. Spillantini, invited talk at TAUP97 in *Proceedings of TAUP97*, edited by A. Bottino, A. Di Credico and P. Monacelli, *Nucl. Phys.* **B70** (Proc. Suppl.) (1999) 545–551.
9) H. Matsunaga, Ph.D. thesis, University of Tokyo, 1997; H. Matsunaga *et al.*, *Phys. Rev. Lett.* **81** (1998) 4052 ; S. Orito, Talk given at the 29th International Conference on High-Energy Physics, Vancouver, July 1998.
10) AMS Collaboration 1994 "Alpha magnetic spectrometer for extraterrestrial study of antimatter, matter and missing matter on the international space station alpha" proposal; S. Ahlen *et al.*, *Nucl. Instrum. Methods* **A350** (1994) 351.
11) R. Bellotti *et al.*, "PAMELA: an antiproton, positron experiment on a polar orbit satellite" (1995) preprint DFF/240; O. Adriani *et al.*, in *Proceedings of the 24th ICRC* (1995) Rome.
12) L.C. Tan and L.K. Ng, *Phys. Rev.* **D26** (1982) 1179 .
13) G. D. Badwar and S.A. Stephens, *Astrophysical Journal* **212** (1977) 494 .
14) Y. Sofue, M. Fujimoto and R. Wielebinski, *Annual Review of Astronomy & Astrophysics* **24** (1986) 459.
15) W.R. Webber, M.A. Lee and M. Gupta, *Astrophysical Journal* **390** (1992) 96 .
16) R.L. Golden, S. Horan and B.G. Mauger, *Phys. Rev. Lett.* **43** (1979) 1196 ; E.A. Bogomolov *et al.*(1979) in *Proceedings of the 16th ICRC* Kyoto; A. Buffington, S.M. Schindler and C. Pennypacker, *Astrophysical Journal* **248** (1981) 1179 ; A. Buffington and S.M. Schindler, *Astrophysical Journal* **248** (1981) L105 ; S.P. Ahlen *et al.*(PBAR Collaboration); *Phys. Rev. Lett.* **61** (1988) 145 ; R.E. Streitmatter *et al.*, *Adv. Space Res.* **9** (1989) 1265.
17) T.K. Gaisser and R.K. Schaefer, *Astrophysical Journal* **394** (1992) 174 .
18) P. Chardonnet, G. Mignola, P. Salati and R. Taillet, *Phys. Lett.* **B384** (1996) 161 .
19) Ficenec *et al.*in *Proceedings of the 23rd ICRC*, editors D. Leaky, R. Hicks and D. Venkatesan, World Scientific **1** (1994) 515.
20) A.G. Lyne, R.N. Manchester and J.H. Taylor, *Mon. Not. R. Astron. Soc.* **213** (1985) 613.

21) G. Jungman, M. Kamionkowski and K. Griest, *Phys. Rep.* **267** (1996) 195 .
22) D. Reusser *et al.*, *Phys. Lett.* **B255** (1991) 143 ; R. Bernabei *et al.*, *Phys. Lett.* **B389** (1996) 757 .
23) R. Bernabei *et al.*, preprint `astro-ph/9710290`.
24) L. Bergström, J. Edsjö and P. Ullio, `astro-ph/9902012` (1999).
25) J.W. Bieber *et al.*, `astro-ph/9903163`.
26) D. Maurin (1999) in preparation.
27) M. Simon and U. Heinbach, *Astrophysical Journal* **441** (1995) 209 .
28) U. Heinbach and M. Simon, *Astrophysical Journal* **456** (1996) 519 .
29) I.V. Moskalenko, A.W. Strong and O. Reimer, Astrononomy & *Astrophysics* **338** (1998) L75 .
30) M. Simon, A. Molnar and S. Roesler (1997) in the *Proceedings of the 25th ICRC* Durban 265.